NASA CONTRACTOR REPORT 177467

Evaluation and Application of a New Interferometry Technique for Compressible Flow Research

William D. Bachalo
Michael C. Houser

Contract NAS2-11575
October 1988

National Aeronautics and
Space Administration

NASA CONTRACTOR REPORT 177467

Evaluation and Application of a New Interferometry Technique for Compressible Flow Research

William D. Bachalo
Michael C. Houser
Aerometrics, Inc.
894 Ross Drive
Sunnyvale, CA
94089

Prepared for
Ames Research Center
Contract NAS2-11575
October 1988

National Aeronautics and
Space Administration

Ames Research Center
Moffett Field, California 94035

ABSTRACT

A new method for obtaining large scale interferograms of flow fields in real-time was investigated. The method was based upon the point diffraction interferometry technique. This method was modified to accommodate the higher laser power required in recording transonic and supersonic flow fields. Basic tests were conducted in unsteady flows and flows about circulation control airfoils at transonic speeds. It was found that vibration was not a significant factor in the application of the system. In the case of the circulation control airfoils, the real-time viewing allowed the identification of the Coanda jet interaction with the external flow and the shedding of large scale vortices. The method proved to be very sensitive to the optical quality of the wind tunnel windows. The results obtained were compared with earlier interferograms obtained using interferometry. These results were in qualitative agreement.

1.0 INTRODUCTION

The application of optical interferometry to research in compressible flows, heat transfer, plasma dynamics and other disciplines has succeeded in demonstrating the capabilities and value of the diagnostic technique. Interferometry provides a means for measuring the variations in the refractive index field of transparent media by determining the changes in the optical path length through the media. Because the refractive index of a medium is dependent upon the density as well as other properties, interferometry can be used to obtain this information. The method has the advantages of obtaining the information nonintrusively, recording the information instantaneously, and providing global flow visualization and quantitative results. These characteristics are especially useful in the research of unsteady transonic flows.

Transonic flow fields are well suited to the application of interferometry since the flows are very sensitive to perturbations by material probes and the gas density varies continuously throughout the flow field with the exception of shocks. The shocks are generally weak so the assumption that the flow is isentropic is valid. The interferograms produce a detailed mapping of the flow field and the quantitative results obtained have been shown to produce an accurate representation of the flow properties.[1] These results included both the inviscid and viscous flow data. The strong coupling between the inviscid and viscous phenomena in transonic flows predicates the simultaneous observation of the global features of the flow fields and the local viscous-inviscid interactions. Conditions

such as the shock boundary layer interaction, turbulence-induced compression waves, and pressure gradients generated by the model profiles influence the character of the entire flow field. The ability to instantaneously record the flow characteristics over the entire field of view is a significant advantage when applied to unsteady compressible flows which include oscillating airfoils, oscillating flaps, and helicopter rotor flow research.

There are many applications in which the immediate observation of the visualization results would be very useful. Although such flow visualization in the form of the shadowgraph and Schlieren techniques are generally available, the additional quantitative information available from interferometry would be of value. For example, this capability could be utilized in the selection of flow conditions, determining hysteresis effects in unsteady flows and the setting of suction rates on adaptive wall wind tunnels as well as studying unsteady two- and three-dimensional flows.

Interferometric information may be used with tomographic techniques to reconstruct general three-dimensional density fields. Because the interferometer integrates the refractive index information along the entire path of the light rays, additional views are required in three-dimensional density fields. Phase shift integral inversion methods are then used to extract the flow field information from the data. Such inversions portend the requirement of recording and handling large quantities of data.

The introduction of holography by Horman[2] and the initial applications to aerodynamic measurements by Heflinger,

Wuerker, and Brooks[3,4] represented a notable advance in terms of where the method could be applied. Holographic light wave reconstruction and pulsed lasers provided the means through which the limitations associated with vibration and optical quality were essentially eliminated.

These results suggested the possibility of utilizing the method in large scale wind tunnels. This allowed a much greater range of applications for interferometry. A notable accomplishment was the successful implementation of the technique in large scale wind tunnels and helicopter rotor facilities[4,5,6] where optical path lengths were necessarily long, vibration levels were high and compromises in the optical components were necessary. The need to record large numbers of interferograms in unsteady and three-dimensional flows and the desire to obtain results in real-time, however, sets the holographic techniques at a disadvantage. Problems emerge with the method because of the time required in aligning the system, recording the results, and the number of steps required to process and reconstruct the interferograms. The double plate method generally required in obtaining quantitative results in moderate to high vibration level environments can be especially tedious. Unless the user of the system is highly skilled and familiar with the fluid mechanics, gross errors can be made in the application of this method.

A new interferometry technique was conceived and research was directed toward the investigation of its potential for providing real-time interferometry data. The method had the further potential advantages of being easier to implement and the

needed insensitivity to the inevitable vibrations present in most applications. If the method proves to be suitable for fluid dynamics applications, the interferograms could be recorded at rates of the order of 1,000 frames per second using high speed movie cameras, video tape or other, even more direct means. In this report, the method is described in detail and its advantages and limitations presented. Test data are given along with comparisons to holographic interferometry.

2.0 DESCRIPTION OF THE EXPERIMENTAL TECHNIQUES

2.1 Optical Interferometry

Interferometry which utilizes the mixing of two coherent waves for the purpose of measuring the distortion in one of the waves has been widely used and is well understood. The introduction of holography as an intermediary means for recording the light wave information has allowed a good deal of versatility in the technique and has greatly extended the possible applications. A unique and advantageous feature of the holographic techniques is that the interference is between two reconstructed waves that have followed the same (or similar) optical paths but were separated in time. This is unlike the Mach-Zehnder or other methods in which the light waves traverse different paths but interfere at the same time. The difference is important because with the holographic method, errors produced by the imperfections in the optical elements tend to cancel when the waves interfere.

There are several ways in which holography can be used in an interferometry.[1] The dual plate technique has proven to be most useful in fluid dynamic applications wherein quantitative results were required. This interferometry method has been demonstrated[5,6] to be a very useful tool in obtaining global visualizations and accurate quantitative data in compressible flows. Examples of interferograms obtained in the NASA Ames 2-by-2-foot wind tunnel with this method are shown in figures 1a, b, c, and d. As part of the development task, quantitative results were obtained from the interferograms and compared to measurements obtained using other means. In two-dimensional flows, the process in obtaining information on the flow properties is

simple. The density is obtained from the fringe data using the relationship

$$\rho(x,y) = \rho_o + \frac{N\lambda}{KL} \tag{1}$$

where ρ and ρ_o are the densities at two locations, N is the fringe shift between the locations, L is the width of the test region, λ is the laser wavelength, and K_{GD} is the Gladstone-Dale constant relating the refractive index to the specific fluid density at wavelength λ. When aligned in the infinite fringe mode, each fringe represents a constant density contour. With the assumption of isentropic flow, the densities can be reduced to surface pressure coefficients by the relationship

$$\frac{P}{P_t} = \left(\frac{\rho}{\rho_t}\right)^{\gamma} \tag{2}$$

and

$$C_p = \frac{2}{\gamma M_\infty^2}\left[\left(\frac{P}{P_t}\right)\left(\frac{P_t}{P_\infty}\right) - 1\right] \tag{3}$$

where M_∞ is the freestream Mach number, $\gamma = 1.4$, and P_t and ρ_t are the total pressure and density. Comparisons of the measured surface pressure and the interferometric data were made, figure 2, to demonstrate the reliability of the method in measuring transonic flows. Good agreement was achieved even under severe flow separation.

Obtaining the pressure data with an interferometer has several advantages. Because some models are difficult to instrument, a significant savings in model costs may be realized. Furthermore, the static pressures may be obtained beyond the trailing edge of the airfoil or anywhere else in the flow field. This presents the possibility of using interferometry to monitor

the flow quality and assess the wind tunnel wall effects. Current interest in wind tunnel wall effects and the introduction of adaptive walls will require a means to evaluate the flow rapidly and direct the changes to the wall contours and/or suction.

The flow speed may also be calculated from the measured density distribution using the following relationship:

$$\frac{V}{C} = \left[\frac{2}{\gamma-1}\left(1 - \left(\frac{\rho}{\rho_t}\right)^{\gamma-1}\right)\right]^{\frac{1}{2}} \tag{4}$$

where C is the speed of sound at stagnation conditions. Figure 3 shows the comparison of the flow speed obtained from the interferometer and the laser Doppler velocimeter. At 6.2^{o} angle of attack, the laser velocimeter showed a progressive increase in the difference of the results in the regions of strong velocity gradients. It is possible that the particles used in the LDV measurements were not tracking the strong acceleration and decelerations of the flow. It is also possible that there was a normal pressure gradient causing the velocity lag. The magnitudes agree very well upstream of the leading edge, at the peak flow speed and on the aft portion of the airfoil where the flow speeds were relatively constant.

Boundary layer and wake density profiles were also determined from the interferograms and compared to pitot and LDV data.[5] The viscous profiles were obtained using the Crocco relationship

$$\frac{T}{T_e} = 1 + r\frac{\gamma-1}{2}M_e^2\left[1 - \left(\frac{U}{U_e}\right)^2\right] + \frac{T_w - T_{ad}}{T_e}\left(1 - \frac{U}{U_e}\right) \tag{5}$$

and the perfect gas law. T_e, T_{ad}, and T_w are the edge, adiabatic and wall temperatures, respectively. The good agreement shown in figure 4 confirms the ability to obtain accurate mean density profiles in the viscous layer even in separated flows. Assurance that the mean viscous flow characteristics can be determined reliably using interferometry, suggests that the technique may be very useful in obtaining complete characterizations in unsteady flow research.

Currently, the use of holography limits the general use of interferometry in obtaining flow field data because the method is time consuming and difficult to apply and does not always produce high quality noise-free interferograms. Thus, the technique does not lend itself to the automation of the data reduction process. In addition, the method would be much more valuable if the flow visualization and ultimately, the quantitative results were immediately available. Although it is not a serious limitation, the alignment of the holographic system in large scale facilities can be difficult and frustrating. This is particularly true for the reference beam. Any method that alleviates these limitations would be a significant achievement and would then allow a more general use of this diagnostic technique.

2.2 Real-Time Interferometry

Although holographic interferometry has the aforementioned disadvantages, it remains as the only available method capable of producing quantitative interferometric data in large scale wind tunnels. Other techniques such as shearing, diffraction,

and Michelson interferometry have been used to provide real-time information on time-varying phenomena, but these methods cannot produce generalized quantitative results. These methods produce the interference between waves that pass through the test field on optical paths which are displaced with respect to each other. For example, the shearing interferometer uses a thick beam splitter to offset the image to produce interference between slightly displaced (order of 25 mm) regions of the flow field. In very small scale facilities, the Mach-Zehnder has been used to produce high quality infinite fringe interferograms in real-time. The ability to record the information at a high framing speed has allowed documentation of the types of instabilities which lead to oscillations of subsonic, transonic, and supersonic duct flows.

Both steady and unsteady flow research on compressible flows would benefit if real-time interferometry was available. For example, overall flow field unsteadiness is of concern in shock boundary layer interactions in otherwise steady flows. Under stalled conditions, quasi-periodic shedding of two-dimensional vortices may occur and hence, have an impact on the development of the prediction methods. Unsteady flows may be recorded by instantaneous exposures at the various phase angles under the assumption that there is no cycle-to-cycle variation. However, it would be more efficient and desirable to record the information at high rates over a single cycle.

2.3 Point Diffraction Interferometer

A relatively new interferometry technique has been developed for testing large optical components. The method was

recognized as having the potential for providing real-time interferometric results in compressible flow applications. The point diffraction interferometer (PDI) as described by Smartt,[7] is like some other forms of radial shear interferometers insofar as it has the unique configuration wherein the light is divided into two components to produce the test and reference waves, after passing through the test field. However, the PDI is the only known concept capable of producing the quantitative information on the light wave distortion directly.

With the PDI, the spherical reference wave is generated by diffraction at a point discontinuity located in the path of the beam. The discontinuity can be either a circular aperture, an opaque disk, or spherical particles. Figure 5 illustrates the principle of operation. The aperture (or opaque disk) is located at the image of the wave front to be analyzed. In the embodiment proposed by Smartt, an aperture in an absorbing film or an otherwise nondiffracting substrate was used. Light incident upon the film and aperture is transmitted with a reduction in amplitude while the aperture produces a spherical diffracted wave. If the aperture is sufficiently small, a spherical diffracted wave is produced which will interfere with the entire transmitted test wave.

Movement of the aperture along the optical axis away from the focal plane will produce circular fringes. Lateral movement of the aperture can be used to produce linear fringes for finite fringe operation. Deliberate displacement of the aperture will reduce the intensity of the diffracted wave which, in turn, reduces the visibility of the resulting fringes.

The important parameters affecting the visibility or contrast of the resulting fringes are the aperture size and the relative film and aperture transmittances. The cone angle defined by the first minimum in the diffraction pattern should be greater than that of the receiver system. These requirements can be satisfied with the proper selection of the aperture size. However, in the special case of fluid dynamics applications where the wave distortions are expected to be large, the fulfillment of these requirements will become more difficult.

Another requirement that is specific to fluid dynamics applications is the need for very short duration exposures to freeze the motions in the flow field. Short exposures, in turn, demand the use of high power continuous wave (CW) or pulsed lasers. The use of substrates with apertures or disks cannot withstand such high energy levels. Our preliminary tests demonstrated that even at very low energy levels, the pulsed laser burned holes in the substrates rendering the devise inoperable.

Because of the large range of wave distortions present in fluid dynamics applications, a greater range of amplitudes in the diffracted and transmitted waves will occur. The distribution of energy incident upon the aperture will be significantly reduced when the focused beam is spread as a result of the flow field turbulence and refractive gradients in the inviscid flow. With relatively weak disturbances to the wave fronts, a greater amount of energy will be focused onto the aperture resulting in a greater amplitude in the diffracted wave. The resulting changes in the amplitudes of the focused beam will produce large variations in the relative intensities of the object and reference

waves which will reduce the visibility of the interference fringe pattern, possibly to an extent where the pattern may be imperceptible. Some of these difficulties can be corrected by changes in the size of aperture and the relative absorption of the substrate. However, if the aperture is too large, the diffracted cone of light will be too narrow and some of the distorted wave may appear on the diffracted wave. By increasing the absorption of the substrate, the possibility of burning it out is increased, and there may be insufficient energy for the high speed recordings.

Clearly, the advantages of the technique which included relative simplicity of operation, insensitivity to vibration, and the opportunity for real-time recording suggested that attempts to modify the concept were worthy of attention. The aforementioned limitations to the application of the method in fluid dynamics research may be solved by redesigning the optical configuration. The operation and stability requirements of the proposed concept should be very similar to the constraints associated with a Schlieren system.

2.4.1 Analysis

The complete understanding of the point diffraction interferometer technique requires the theoretical analysis of the phenomena involved. An estimate of the phase shifts or wave distortions to be expected was obtained from our previous work in holographic interferometry.

The description of the amplitude and angular distribution of light scattered by a circular aperture can be approximated by the Fraunhofer diffraction theory as

$$I_{sca}(\Theta, d) = I_0\left(\frac{\pi d^2}{4\lambda}\right)^2\left[\frac{J_1\left(\frac{\pi d}{\lambda}\sin\Theta\right)}{\left(\frac{\pi d}{\lambda}\sin\Theta\right)}\right]^2 \qquad (6)$$

where θ is the scattering angle measured from the transmitted beam, I_0 is the incident beam intensity at the aperture, d is the aperture diameter, λ is the laser wavelength, and J_1 is the first order Bessel's function of the first kind. Using this expression, the diffraction pattern can be matched to the numerical aperture of the collimating lens L6 of figure 6. An estimate of the relative intensities of the reference and object wave was also made.

The size of the aperture is of importance for its efficacy as a low pass spatial filter and for producing a spherical wave front of sufficient intensity. The intensity of the beam is proportionate to the square of the aperture diameter (d^2), whereas the angular distribution is inversely proportional to the diameter (1/d). Thus, an increase in the aperture diameter by a factor of 2 results in an intensity increase by a factor of 8. However, the aperture must be small enough to remove the high frequency information generated by the flow field. Increasing the focal length of the focusing lens on the reference beam can alleviate this problem, but with a corresponding loss in intensity incident upon the aperture. When a very small aperture is used with a highly focused beam, there is an added potential for burning out the aperture and beam drift

becomes more serious. When optical movement or the flow field slightly deflects the beam, the peak intensity will move from the aperture causing intensity fluctuations on the reference beam. In a properly designed system, the object and reference waves are deflected together. Thus, the angle of the wave fronts will not change, so the interference patterns will not generate significant error.

In order to evaluate the system, experiments were conducted which consisted of introducing phase shifts in the beam, optically filtering it and then interfering the filtered wave with a test wave that was spherical or planar as appropriate. With this procedure, the filtering was evaluated under controlled levels of distortion on the incident waves. The relative transmission efficiency was measured. Several combinations of transform lenses and apertures were considered in the analysis. The controlling parameter was the intensity incident upon the pinhole. A short focal length lens increased the intensity and accelerated the burnout of the pinhole. On the other hand, a long focal length lens and larger pinhole required a much longer focal length lens to collimate the filtered reference beam at a diameter large enough to overlap the object or data beam. Deflected rays were then traced through the optical system using the laws of geometrical optics. In this manner, the optics system was refined.

An additional consideration is the possibility of vignetting of the object wave to produce a Schlieren effect. The light wave passing through the flow field is deflected by refraction and diffraction. The optics in the path of the object wave

must admit all of the deflected as well as the undeflected light. With compressible flows, the greatest deflection occurs in boundary layers, wakes, at shocks and at the leading edge of airfoils. Past experience was used to calculate the expected deflections. For example, a boundary layer with 50 fringes per centimeter will produce a deflection angle given as

$$\theta_d = \text{atan}\left(\frac{n\lambda}{L}\right) \tag{7}$$

where n is the number of fringes, λ the optical wavelength, and L the dimension normal to the fringes. For the above example, $\theta_d = 0.15^o$ which is relatively small except when propagating over large distances. In general, optics of sufficiently small f/no. will perform satisfactorily. That is, the f/no. should be smaller than the f/no. of the Schlieren mirrors or lenses used to collimate the light through the test section.

One disadvantage of the present method is that all optical components must be of very high quality. The aperture or diffraction element forms an ideal spherical wave if it has a circular cross section. Hence, the undisturbed wave passing through the system must also be spherical. Distortions introduced by the optics in the form of coma, spherical aberrations, and astigmatism will generate spurious fringes. In fact, the original application of the technique was to measure such optical defects. Fortunately, before each application, the optics can be evaluated by observing the fringe patterns formed without the flow field. If the fringes are not concentric circles or linear fringes, one or more of the defective optical components must be replaced.

Most Schlieren systems use parabolic or spherical mirrors in an off-axis Z configuration. Although this configuration minimizes astigmatism, it still presents problems for the present method. The recollimated light waves will not be planar so the interference pattern cannot be aligned to the infinite fringe mode. A cylindrical lens may be inserted in the divergent beam just beyond the light source to compensate for the astigmatism. Off-axis parabolic mirrors may also be used, but such mirrors are very expensive. In the present case, the Schlieren mirrors were used on-axis with a small mirror used to turn the diverging beam onto the mirror optical axis. This method has the disadvantage of the mirror appearing in the field of view.

Estimates of the fringe spatial frequencies and light intensities were used in the early stages of the investigation to determine characteristics required of the recording media. Polaroid, 4" X 5" sheet, 16 mm movie, and 35 mm were considered. Requirements on the film resolution were estimated based upon the previous work with holographic interferometry. For example, the fringe spacing in the boundary layer of a supercritical airfoil was approximately 0.5 mm. If the entire field of view was recorded (450 mm), the approximate resolution required for a 4" X 5" film would be 10 lines per mm. On 35 mm, this represents a spatial resolution of approximately 60 lines per mm, which is at the resolution limit of conventional films. High speed film generally has large grain size and lower resolution.

2.4.2 Improved Point Diffraction Interferometer

A great deal of flexibility in the operation of the method was achieved with the optical configuration shown in figure 6.[8] The layout of the system is the same as for a Schlieren system up to the receiver section. Either a CW or pulsed laser may be used as the light source. The light beam is spatially filtered and expanded to fill the lenses or mirrors of the transmitter system and form a collimated beam. The field to be tested is located in the beam path, as with a conventional Schlieren system. The receiver mirror serves to focus the light after it passes through the test section. At the receiver, the beam is split into two optical paths with a beam splitter. The transmitted beam is spatially filtered to remove the high spatial frequencies which are produced by the refractive field in the test section. This diffracted beam will act as the reference wave. The reflected beam retains the wave distortion information produced by the refractive field. It is then recombined with the reference wave. The system can be aligned in the same manner as a common Mach-Zehnder interferometer. However, optical components on the receiver section can be made very compact and are rigidly mounted such that vibration need not be more serious than for a Schlieren system.

Inasmuch as this configuration complicates the technique, it also offers the needed flexibility in the application of the method to fluid dynamics investigations. First of all, the use of two separate paths allow the reduction of energy incident upon the aperture. The aperture can now consist of pinholes that will withstand the high energy levels and which are

commercially available. Because of the losses involved in the filtering process, a variable beam splitter can be used instead of an absorbing substrate to maximize the use of the available light. Additional attenuation may be introduced to maximize the visibility of the interference fringe pattern and hence, the signal-to-noise ratio. Both the transmitted and reflected images of the beam splitter may be used. One image can be used for real-time viewing and while the other is being recorded.

After preliminary development and testing, the optical configuration of figure 6 evolved as optimum for the experimentation to follow. Figures 7a and 7b are photographs of the transmitter and receiver optics. The scale of the system can be estimated from the one-inch center hole pattern on the table. Transmitter and receiver modules were arranged on individual optical benches. These optics were designed to accommodate existing Schlieren systems with little or no modifications.

Referring to figure 6, lens L1 was selected to overfill the Schlieren mirror which was approximately f/10. M2 and M5 were 25 mm in diameter. These mirrors were aligned on-axis to prevent astigmatism. The Schlieren mirrors were from 25 to 50 cm in diameter depending upon the existing wind tunnel optics. Argon lasers having 4 watts and 18 watts of power were used as the light source. On the receiver stage, the Schlieren mirror M4 collected and refocused the light. Lenses L2 (f = 10 mm) collimated the light before entering the beam splitter BS1. BS1 was a coated optical flat with 95% transmission. Approximately 5% of the light was reflected to form the object beam. L3 (f = 100 mm)

and L4 (f = 380 mm) were used to image the test field to the image plane while producing a collimated beam. These lenses were later eliminated from the system and replaced with an imaging lens L7 beyond the beam splitter BS2. The light transmitted through BS1 was focused with lens L5 (f = 100 mm) onto the spatial filter aperture or pinhole which was 20 micrometers in diameter. The spatial filter was mounted on a micrometer-controlled x-y traverse. Lens L6 (f = 380 mm) was used to collimate the diffracted light. BS2 was a 50-50 beam splitter used for recombining the object and diffracted reference beams. The mirrors and beam splitters had x-y adjustment capability to simplify the system alignment. Lens L5 and L6 were on translation bases to allow accurate focusing to the aperture and collimation of the diffracted light.

In addition to the Argon-ion laser, the Quanta Ray Nd:YAG frequency doubled laser used for holography was available. This laser provided high energy (50 millijoule) light pulses of 20 nanosecond duration. Unfortunately, the extremely high beam energy caused the aperture to fail after relatively few exposures to the beam. Hence, this laser was considered to be unsuitable. A pulsed laser with a longer pulse duration on the order of microseconds is more desirable. This would provide sufficient exposure to the film while involving lower energy on the aperture.

The continuous wave Argon-ion laser was used with mechanical camera shutters or choppers. Shutter speeds from 50 to 500 microseconds were used to "freeze" the fringe motions and to provide adequate exposure on the recording medium. Various

types of recording media were employed during experimentation. A Graphic View camera with a 4" X 5" back provided a satisfactory means of viewing the field and aligning the interferometer. Both Polaroid and Ektachrome sheet films were used to record the images. To take advantage of the real-time nature of the interferometer, a Millikan high speed movie camera was used to record dynamic events. In effect, every frame of the motion picture is a complete interferogram in itself containing quantitative information on the flow field under investigation. The motion picture recordings provided the opportunity to view unsteady and changing events during the test run

2.4.3 Experimental Facilities

Indraft Wind Tunnel

The Ames indraft facility has a 13 X 25 cm test section and was outfitted with a NACA 0012 airfoil. The airfoil was affixed to an oscillation mechanism. Oscillation frequencies of 6.25, 12.5, 25.0 and 50 Hz were used during the tests. The tunnel was operated at an inlet Mach number of 0.7. At this Mach number, significant condensation occurred in the test section since room air was drawn into the facility. The facility was equipped with a Schlieren system having spherical mirrors that were 45 cm in diameter.

Ames 2-Foot by 2-Foot Transonic Wind Tunnel

The Ames 2-foot by 2-foot transonic wind tunnel is a closed-return, variable density tunnel with slotted upper and lower test section walls. The slotted walls allow suction to be

applied to alleviate the wall constraints to the flow field. During the tests, the freestream Mach number was varied from 0.5 to 0.9 and the chord Reynolds number from 2 X 10^6 to 4 X 10^6. Several instrumented circulation control airfoils utilizing the Coanda effect were tested. These airfoils had a 15 cm chord and various thicknesses and camber. (This information was deemed proprietary.)

U.C. Berkeley Supersonic Wind Tunnel

The tunnel is a closed-cycle, variable density, continuously operating wind tunnel. By using removable nozzle blocks, test section Mach numbers in the range from M1 = 1.8 to 2.8 can be obtained. The tunnel pressure is adjustable in the range from 2 to 35 psia, and stagnation temperatures are adjustable between 75 and 150 F. The corresponding Reynolds number range is from 0.1 X 10^6 to 10 X 10^6. Width of the test section is 14 cm.

A reciprocating air compressor which loads two storage tanks and a rotary vacuum pump are used to obtain the desired pressure in the tunnel. For operation at stagnation pressures greater than atmospheric pressure, air is bled into the tunnel from the high pressure storage tank. The tunnel air temperature is controlled by an air cooler upstream of the test section. Turbulence is reduced by 6 wire screens (14 mesh, 0.02 in wire, 6 inches apart).

3.0 RESULTS AND DISCUSSIONS

The experiments conducted to evaluate the new interferometer technique were conducted in the various facilities. These results will be presented following the order of tunnel entries.

3.1 Laboratory Testing

The interferometer was first set up in the laboratory and tested using simple flow fields.

The natural convection from a household candle was viewed with the device. Also, the flow from an ignited propane torch was observed. Photographs taken at the interferometer viewing plane are shown in figures 8a and 8b. In both cases, the surrounding undisturbed flow field is shown to consist of only 1 or 2 fringes. This interferometric alignment is referred to as "infinite fringe" mode when very few, if any, fringes exist in the undisturbed portions of the flow. The infinite fringe alignment is also an indication of the overall quality of the interferometer. Optical component imperfections will manifest themselves as spurious fringes which can not be eliminated by interferometer alignment.

Tests conducted in the laboratory involved flow fields that were not confined within a test rig. The question of optical component imperfections must also include test section windows which may add distortion to the transmitted beam. Wind tunnels which have Schlieren flow visualization capabilities usually have Schlieren grade test section windows. The Schlieren optical grade implies very high quality glass which has been

polished for surface flatness and parallelism. A test was conducted in which actual Schlieren quality test section windows were introduced into the object beam while in the laboratory setting. The results showed no beam distortion due to the windows. This no-flow infinite fringe alignment is the definitive test of the component quality of the interferometer.

The final set of experiments performed in the laboratory involved a comparison of the real-time interferometer results with standard dual plate holographic interferometry. The tests involved the natural convection flow around a heated horizontal cylinder aligned with the object beam. Holograms were formed by splitting off part of the incident laser beam (before L1 in figure 6) and directing it around the test area. This beam became the reference beam which was mixed with an object beam on the photographic plate to form the holograms. The holographic object beam followed the same path as the real-time interferometer beam through one leg of the receiver beam path--the beam path which included the diffracting pinhole was blocked during holographic recording. This arrangement allowed for rapid changes between holography for rapid conversion between holography and real-time interferometry.

The real-time interferometry results were immediately available at the image plane of the receiver. The holographic interferometry results involved exposure of two plates (one as reference and the other as object) followed by developing and later in vitro reconstruction of the holograms before the interferometric flow visualization was available. Photographic results from both methods are shown in figures 9a and 9b. This

and similar comparisons confirm that the real-time system can produce results identical to holographic interferometry with much less effort. Additional photographs showing the real-time interferometer and holographic interferometry operating in the finite fringe alignment mode is shown as figures 10a and 10b.

3.2 Indraft Wind Tunnel

The optical system was installed on the Ames Indraft Facility using an existing heavy steel plate as the support for the optical tables. This provided a rigid common base between the transmitting and receiving optics. Unfortunately, the Schlieren mirrors were placed on the wooden floor. Individuals walking or standing on the floor produced significant deflections and hence, misalignment of the optics.

A 16 mm Millikan camera operating at 400 frames/sec with shutter speeds of 1/900 and 1/19,200 seconds was used to record the interference fringe patterns. Movies were made with 64 interferograms per cycle at the 6.25 Hz oscillation frequency down to 8 per cycle at 50 Hz.

The recordings obtained were of good quality. A single frame from one such film is shown in figure 11. Since the system was aligned approximately to the infinite fringe mode, each fringe represents a constant density contour. The obscurities in the field of view are the airfoil and oscillator mechanisms. Flow features such as the shocks on the upper and lower surfaces, wake, and inviscid flow field are clearly visualized. It is evident that the wind tunnel walls are constraining the inviscid flow. The movies showed the dynamics of the flow including the

shock motion and development and collapse of the separation. Since room air was drawn into the tunnel at the higher Mach numbers, fog produced significant beam extinction in the test section.

3.3 Ames 2-Foot by 2-Foot Transonic Wind Tunnel

The interferometer was installed at the 2-foot by 2-foot Transonic Wind Tunnel during the testing of circulation control airfoils utilizing the Coanda jet effect. Both the Millikan cameras and still photos were used to record the results. Because of the concrete floor and relatively low vibration levels, the installation and operation was much easier.

An example of the quality of the interferograms may be seen in figures 12, and 13a and b. Figure 12 is the entire flow field for the circulation control airfoil and figures 13a and 13b are enlarged views of the Coanda jet interacting with the turbulent boundary layer. These results obtained with holographic interferometry are similar to those observed using the real-time interferometer.

A great deal of data was obtained and recorded using the real-time interferometer. Unfortunately, because of the circulation airfoil design, most of these data were classified as proprietary and are thus unavailable for this report. The method proved to be valuable as a means for viewing the dynamic behavior of the flow field. Motion of the fringes due to flow field unsteadiness was not so rapid as to cause blurring. Unlike a snapshot that captures the instantaneous details of the flow, real-time viewing provided further visual information on the

unsteady features in the flow. For example, the Coanda jet produced large scale vortex shedding under certain parametric conditions. An even more important observation of the Coanda jet interacting with the incident turbulent boundary layer was easily made.

3.4 U.C. Berkeley Supersonic Wind Tunnel Tests

The objective of this phase of the testing was to make direct comparisons between holographic and the new real-time interferometry method. These comparisons would be made using data obtained in a realistic flow field. Measurements of such features as turbulent boundary layer and flow separation were of interest. Due to the unavailability of suitable wind tunnels at Ames, the U.C. Berkeley Supersonic Wind Tunnel was used.

Figure 14 is a schematic showing the holographic interferometer installed at the facility. Optical breadboards on each side of the wind tunnel were used for mounting the optics. Simple wooden tables were used to support the breadboards. Existing Schlieren mirrors were used to collimate the laser beam at a diameter of 56 cm and direct it through the test section. The second mirror was used to refocus the collimated beam to the receiver system. A reference beam was passed to a plane mirror on the Schlieren mirror stands, directed over the wind tunnel to a second plane mirror on the opposite Schlieren mirror stand and back to the receiver table. The reference beam was expanded to a 9 cm diameter collimated beam that was directed onto the holographic plate to overlap the object beam.

The dual plate method was used in this investigation. Thus, reference plates were recorded with the tunnel off, followed by the data recordings with the tunnel on. A wedge model forming the classic compression corner flow field was used in this study. A 12.5^{o} wedge angle was used and the wedge spanned the test section, but a 1 cm space on each side was provided to minimize the interaction with the sidewall boundary layers. Total pressures of 15, 20 and 25 psia and a Mach number of 2.5 were used.

Figure 15 shows a finite fringe interferogram of the wedge flow. The finite fringes have a slight curvature indicating that the flow was not quite uniform. The boundary layers are clearly visible. An oblique shock formed by the compression corner interacted with the upper surface boundary layer and produced separation. The shock also separated the flow on the wedge. Flow separation appeared to persist to nearly the trailing edge of the wedge. An expansion fan formed at the trailing edge provided the reduction in streamwise pressure gradient needed for the boundary layer to recover. The separated region behind the wedge is visible as S-shaped fringes starting at the outer shear layer.

The improved point diffraction interferometer (PDI) was then installed also using the existing Schlieren mirrors. A photo of the installation is shown in figure 16. In principle, the PDI was easier to install since only a single expanded beam was required. The complex optical alignment was confined to the receiver. At the receiver, the transmitted beam was split into two paths. A focusing lens and spatial filter was used on one

path to remove the disturbances introduced by the flow field. The other beam was passed through the system on a second path, recombined with the first, and directed onto the film plane.

After careful alignment, a hyperbolic fringe pattern remained over the field of view. An example of this pattern is shown in figure 17. Since the optical system had been used in the previous tests and did not show this difficulty, the quality of the Schlieren mirrors and wind tunnel windows were then suspected to be the cause of the optical distortion. Upon careful examination, one of the Schlieren windows was found to be improperly mounted. This window was replaced but the hyperbolic fringe pattern persisted. With both windows removed, a good infinite fringe pattern was obtained. Further testing with one tunnel window at a time revealed that the new window was also producing distortions.

At this point, it was decided to continue the test to establish whether the PDI would work if the window distortions were eliminated. The wind tunnel was turned on and operated at $M = 2.5$ and a total pressure of 15 psia. Some high frequency vibration appeared on the interference fringe pattern. Since the drive motor and blower are on a common concrete floor with the interferometer, this problem was expected. Changes in some of the mounting hardware improved the situation. However, it was determined that reliable testing in that facility will require an air suspension table.

4.0 SUMMARY AND CONCLUSIONS

The improved point diffraction interferometer has been demonstrated to have the capability of producing real-time interferograms in practical wind tunnel environments. In many ways, the method is easier to set up and use than holographic interferometry. It also has the significant advantage of being able to observe the interferograms in real-time much like a conventional Schlieren system. This capability is especially important to the investigation of unsteady flow phenomena. A standard high speed movie camera was found to be adequate in recording the interferograms at rates greater than 400 frames per second.

Because of the high sensitivity of the interferometer, any optical imperfections in the system will produce undesirable fringes. Our experience in the NASA Ames facilities showed that the existing Schlieren windows and mirrors were of sufficient quality for the interferometer. Vibration in the Ames 2-by-2-foot Transonic Wind Tunnel did not create any problems. Unfortunately, this was not true for the U.C. Berkeley Supersonic Wind Tunnel. The setup at U.C. Berkeley would have required a stable table to isolate the interferometer before reliable recordings could be made. It appears that the very thick concrete floor of the Ames tunnel adequately damped the high frequency vibrations.

Another problem was identified which resulted from slight deflections of the beam due to passing through the flow field. For example, if shocks or other localized density gradients were present, the focused intensity on the spatial filter (pinhole) could vary significantly. This caused changes in the reference beam intensity and hence, in the fringe

visibility. A solution to this problem is to use a glass slide with a layer of polystyrene beads to produce the diffracted beam. Another possibility is to use a metal substrate with a relatively high density matrix of apertures of appropriate size. With this arrangement, deflection of the beam will not significantly change the diffracted intensity.

Further work may be required in refining the optics on the receiver. Optics with large enough apertures (small f/#) are required to admit all of the deflected light. Otherwise, the loss of the deflected light will produce blanks in the high density regions of the flow field. A simple ray trace may be used with the estimated maximum deflection due to the flow field to estimate the required lens f/#'s.

In general, the Point Diffraction Interferometer provides a relatively inexpensive yet effective means for obtaining detailed flow visualization and quantitative data in unsteady flows. The method is an alternative to real-time holographic interferometry which remains rather sensitive to vibrations.

References

1. W. D. Bachalo, and D. A. Johnson, "Laser Velocimetry and Holographic Interferometry Measurements in Transonic Flows," Laser Velocimetry and Particle Sizing," Hemisphere Publishing Corp., 1979, edited by H. Doyle Thompson and Warren H. Stevenson.

2. M. H. Horman, "An Applicable of Wavefront Reconstruction to Interferometry," Appl. Opt. 4, 333-336 (1965).

3. L. O. Heflinger, R. F. Wuerker, and R. E. Brooks, "Holographic Interferometry," J. Appl. Phys., 37, 642-649 (1966).

4. R. E. Brooks, L. O. Heflinger, and R. F. Wuerker, "Interferometry With a Holographically Reconstructed Comparison Beam," Appl. Phys. Letters, 7, 1248-249 (1965).

5. D. A. Johnson, and W. D. Bachalo, "Transonic Flow Past a Symmetrical Airfoil-Inviscid and Turbulent Flow Properties," AIAA Journal, 78-117R, Vol. 18, No. 1, January 1980, p. 16.

6. W. D. Bachalo, "An Experimental Investigation of Supercritical and Circulation Control Airfoils at Transonic Speeds Using Holographic Interferometry," AIAA Page No. 83-1793, Danvers, Massachusetts, July 1983.

7. R. N. Smartt, "Special Applications of the Point-Diffraction Interferometer," SPIE, Vol. 192, Interferometry, 1979.

8. W. D. Bachalo and M. J. Houser, "A Real-Time Interferometer Technique for Compressible Flow Research," Paper No. 84-1600, AIAA 17th Fluid Dynamics, Plasma Dynamics and Laser Conference, Snowmass, Colorado, June 1984.

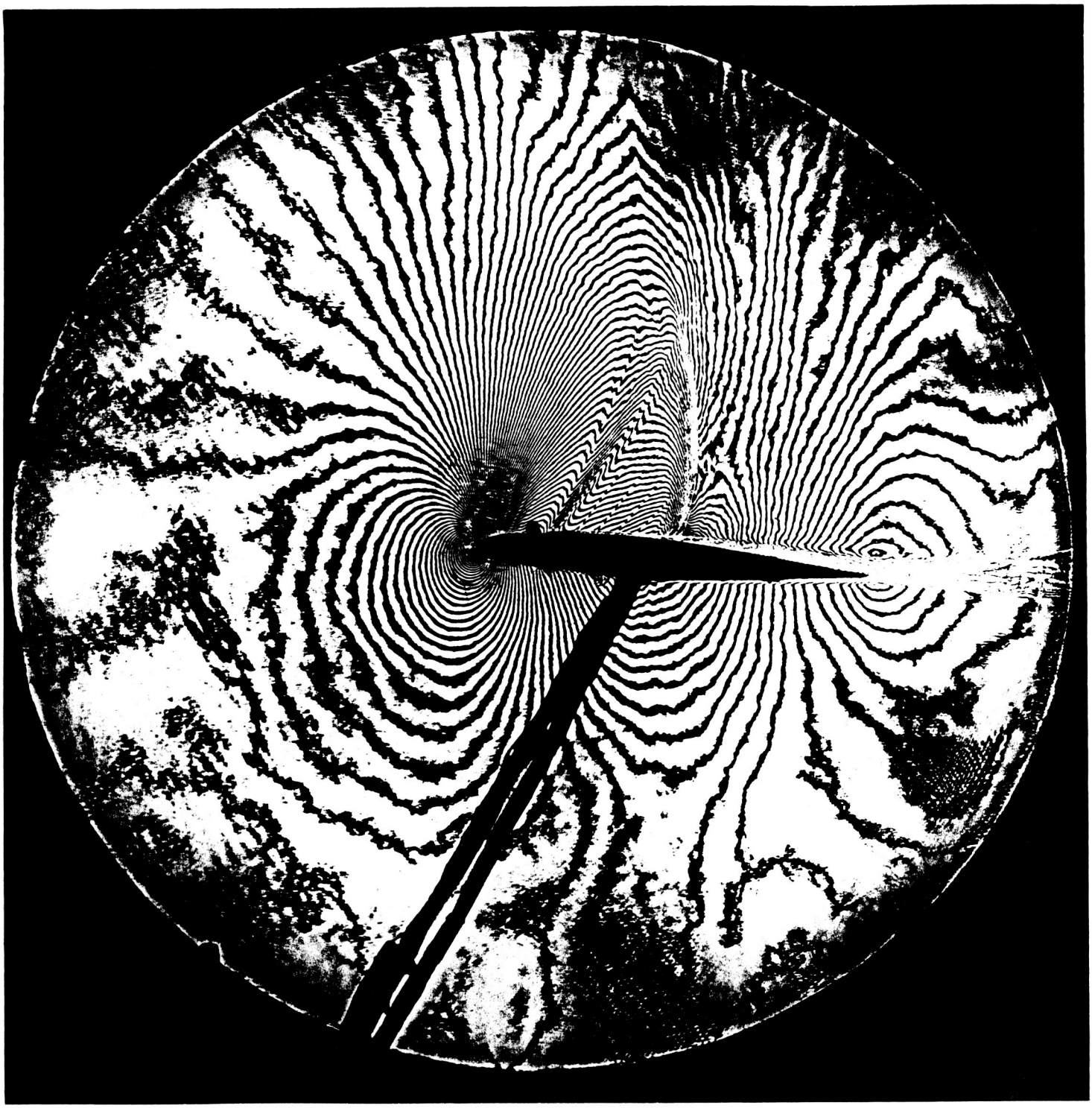

1a. NACA 64010 Airfoil, $M_\infty = 0.8$, $\alpha = 3.5°$

Figure 1. Examples of Holographic Inteferograms of Transonic Airfoil Flow Fields.

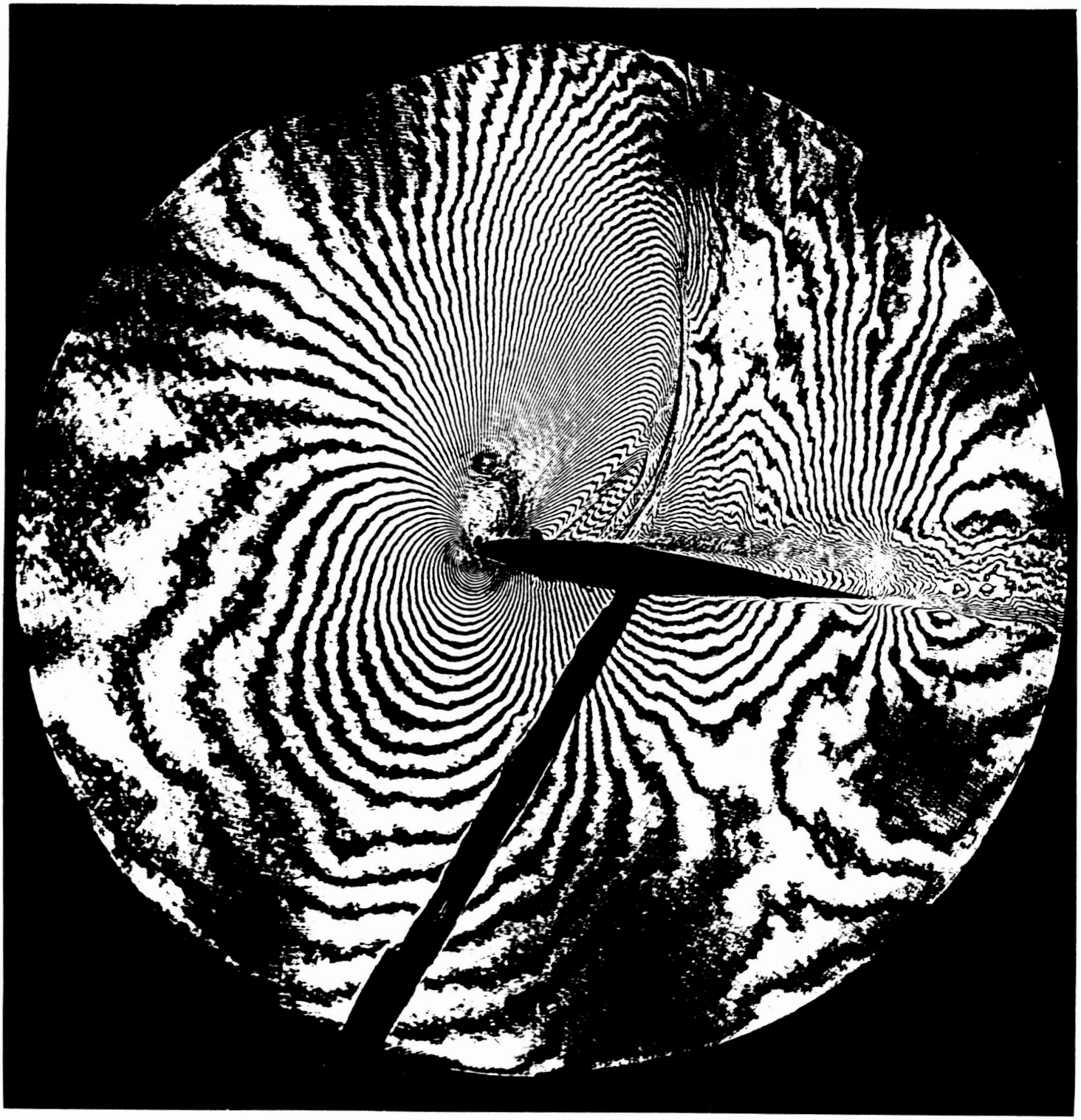

1b. NACA 64010 Airfoil, $M_\infty = 0.8$, $\alpha = 6.2°$

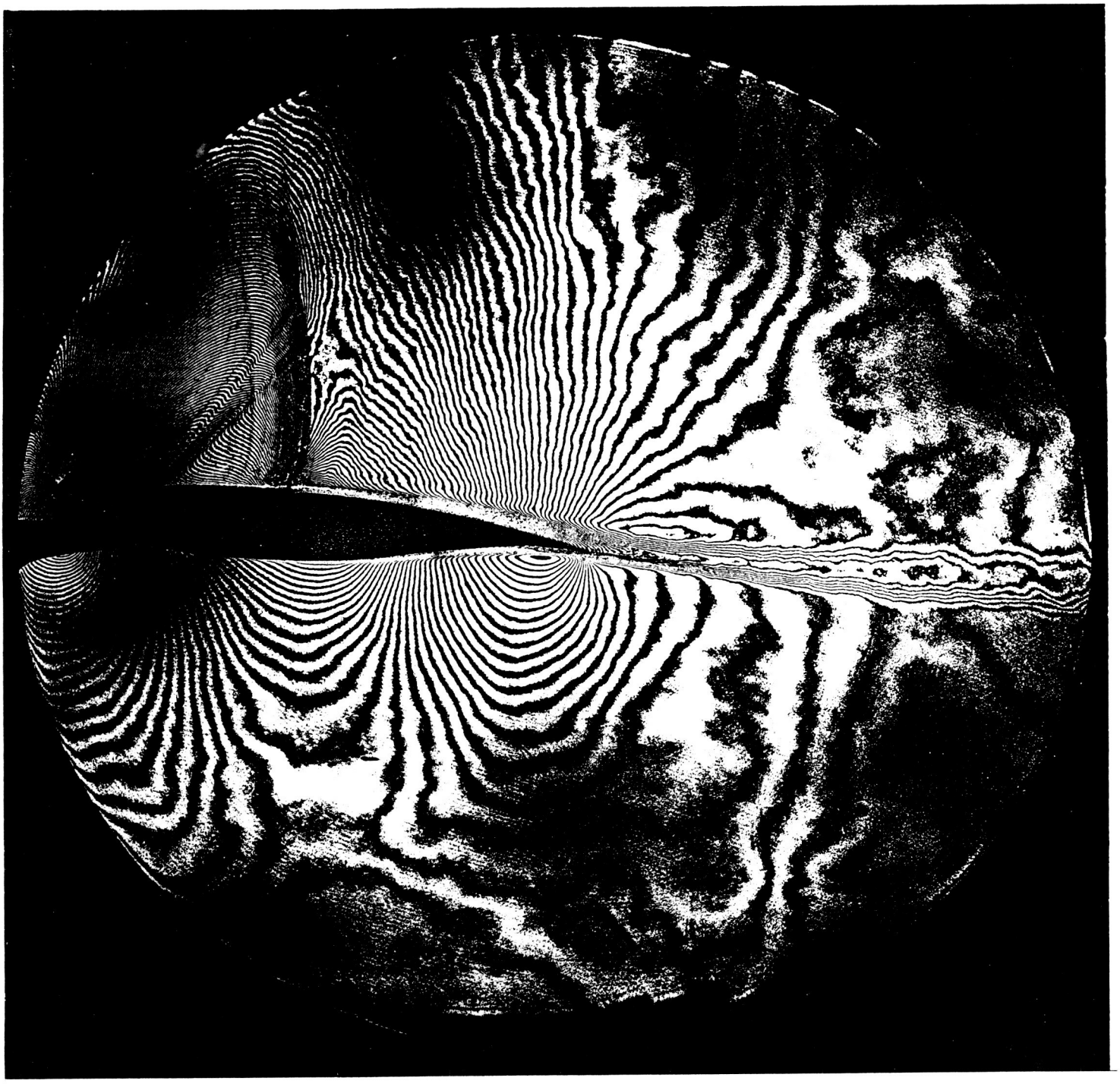

1c. McDonnell Douglas DSMA 671, $M_\infty = 0.72$, $\alpha = 6.10°$

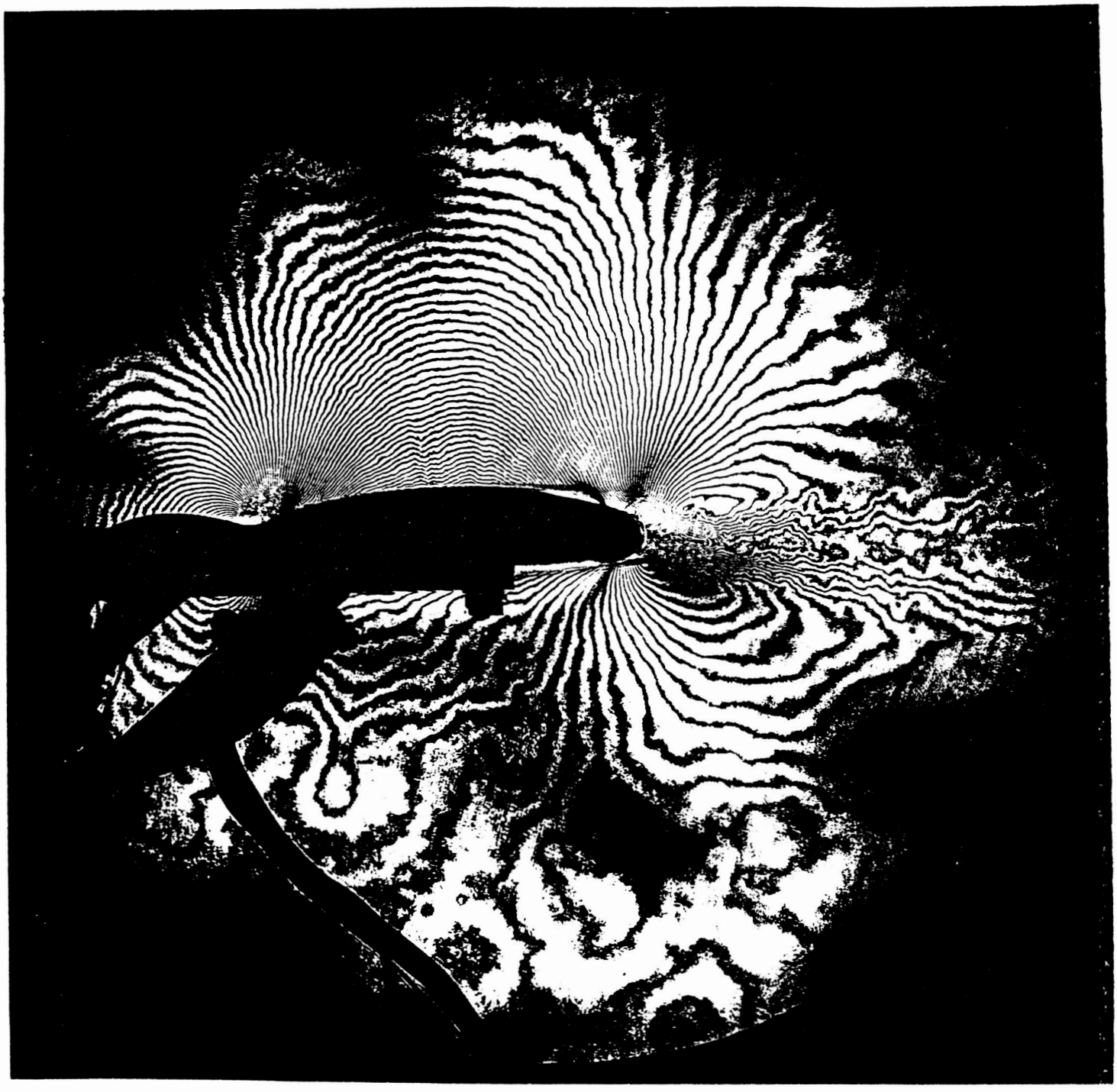

Figure 1d. Circulation Control Airfoil

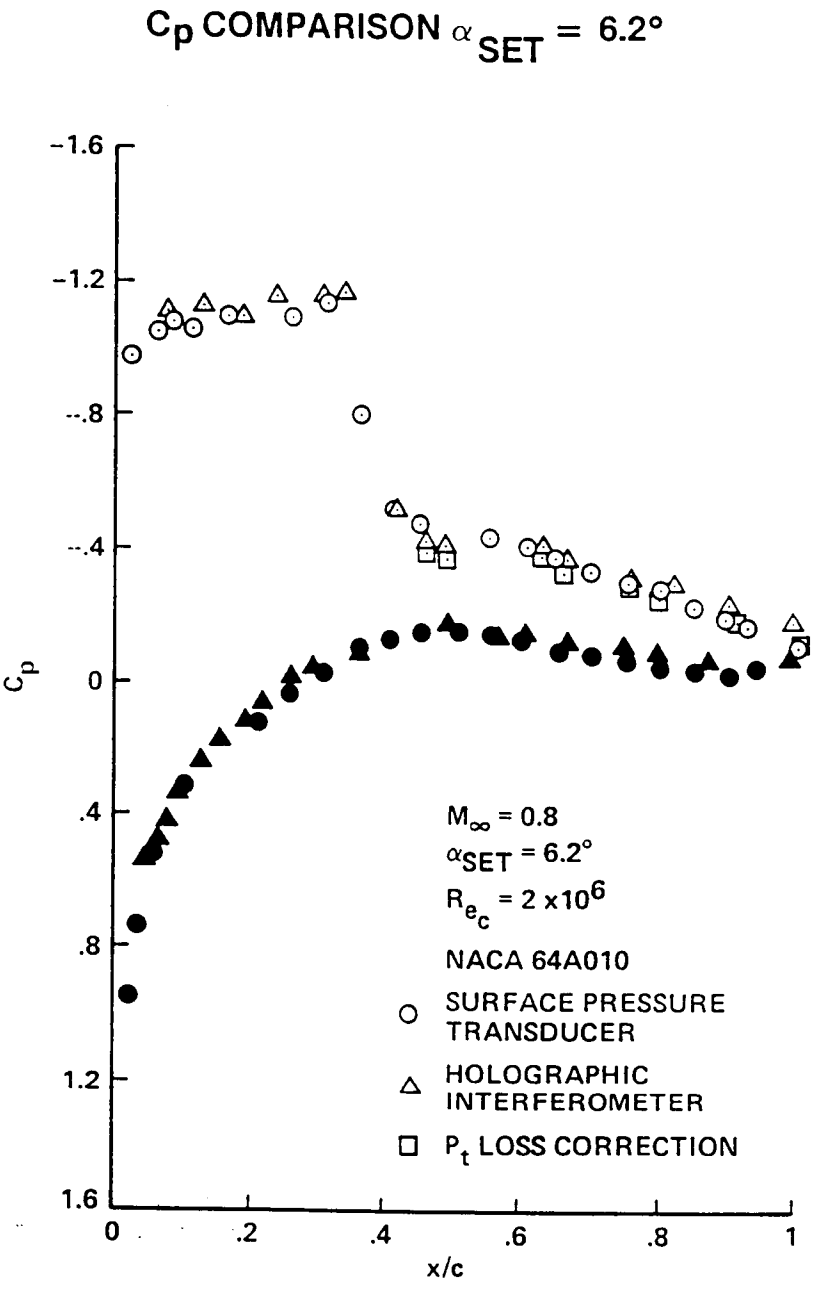

Figure 2. Comparisons of Pressures Obtained with Surface Pressure Taps and Interferometry

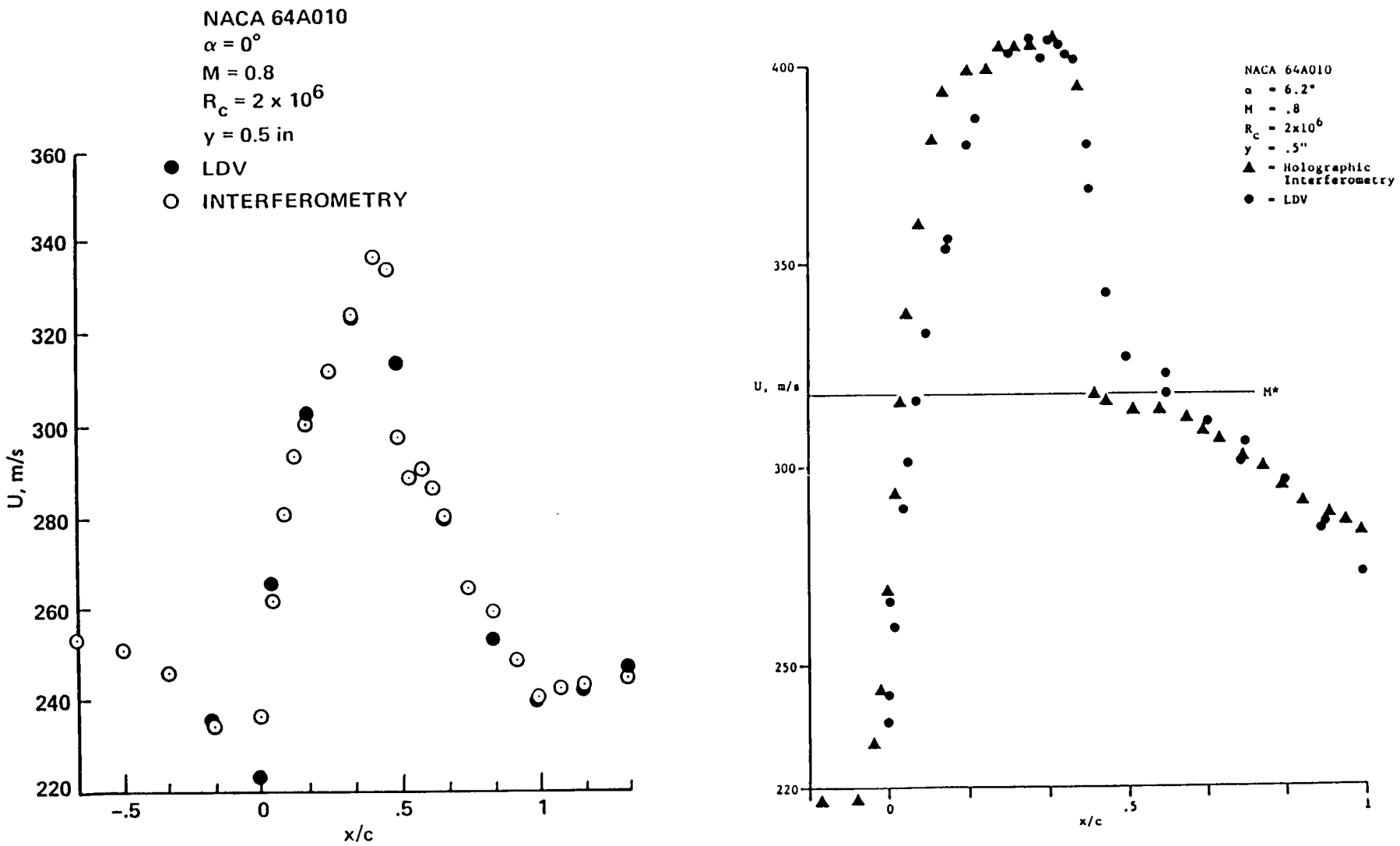

Figure 3. Comparisons of Flow Speed Obtained with the Laser Doppler Velocimeter and Interferometry

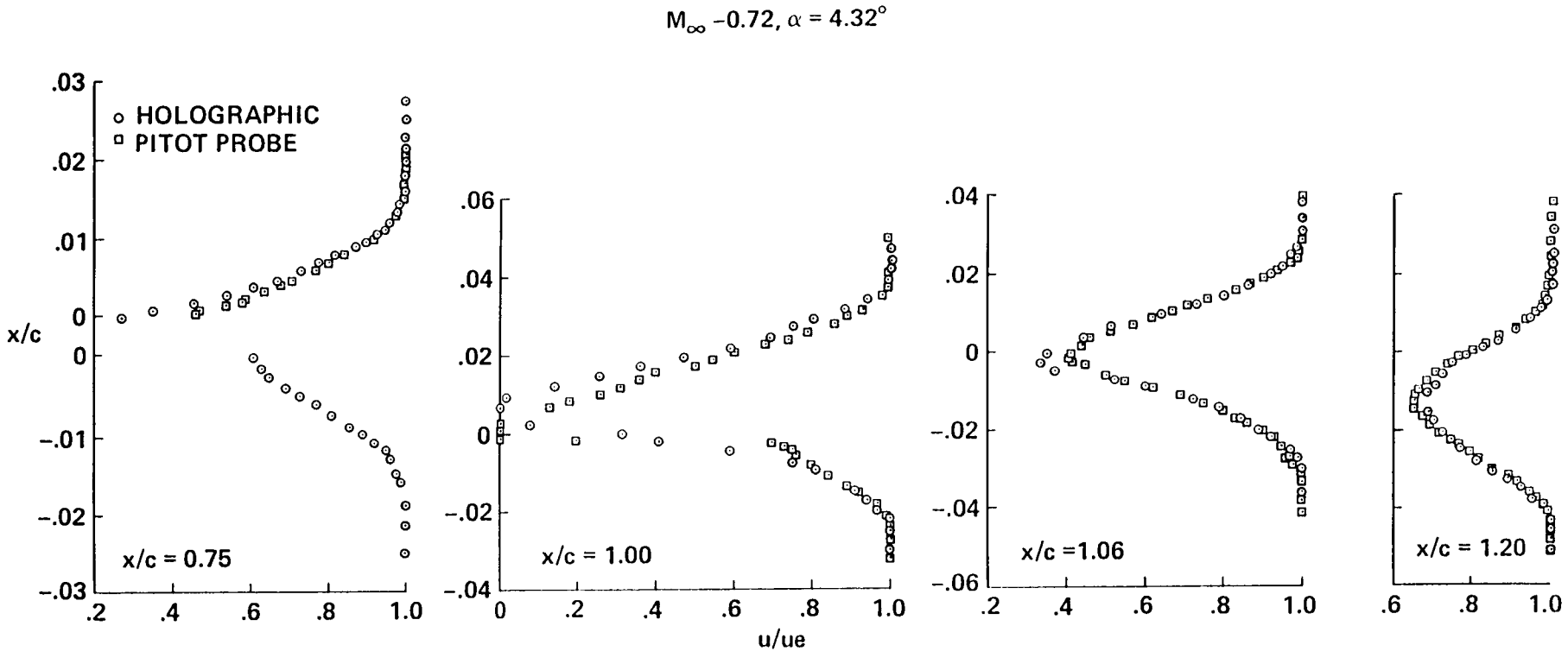

Figure 4. Demonstration of the Ability to Measure Viscous Flows

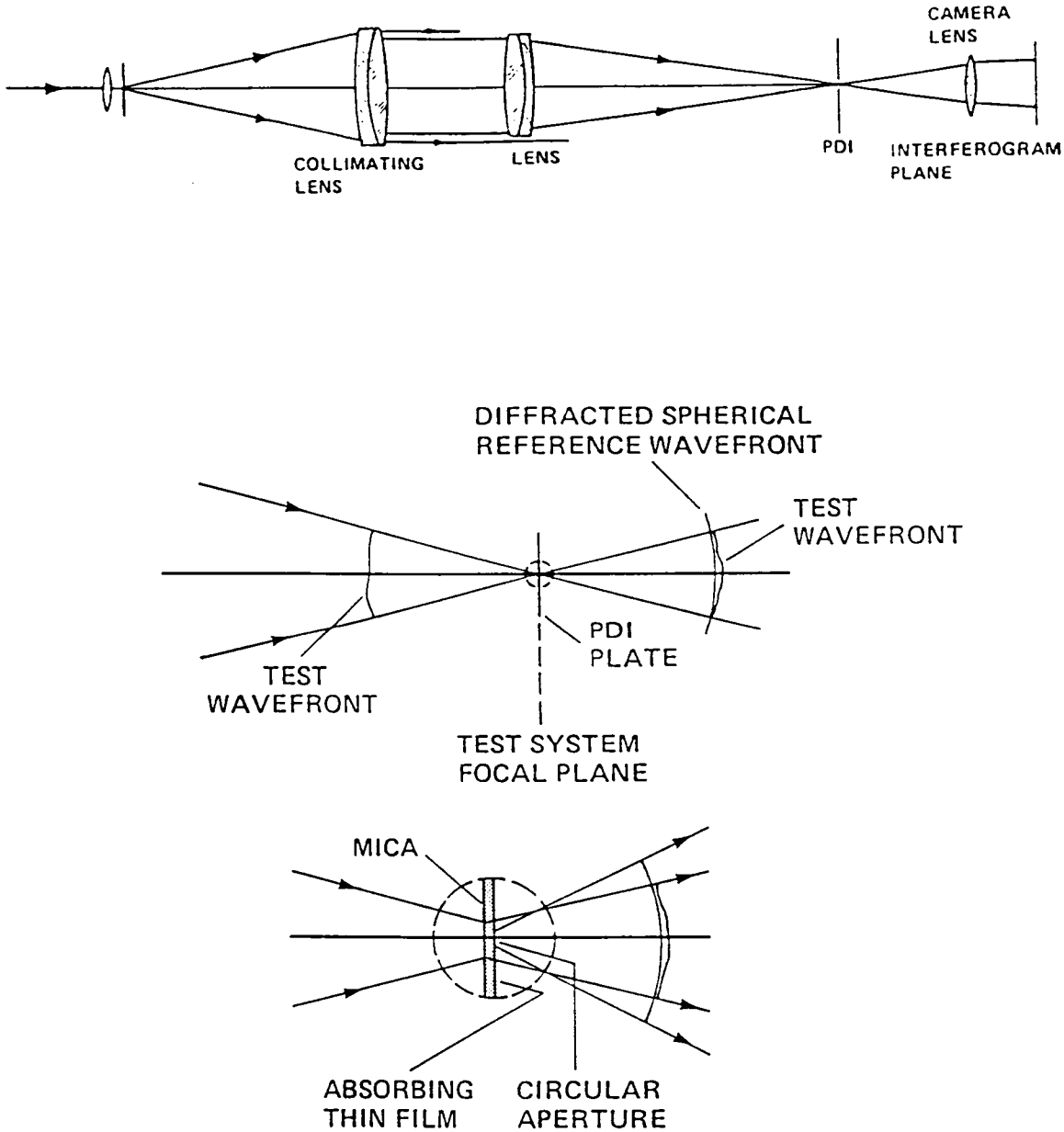

Figure 5. Basic Point Diffraction Interferometer

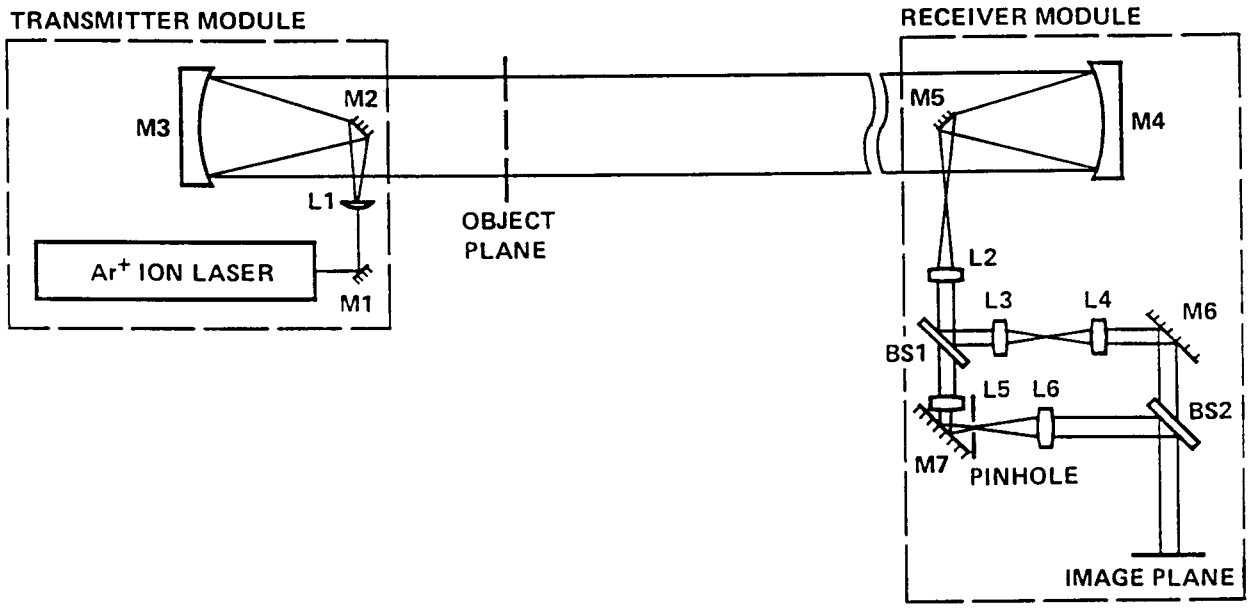

Figure 6. Optical Configuration of the Improved Point Diffraction Interferometer

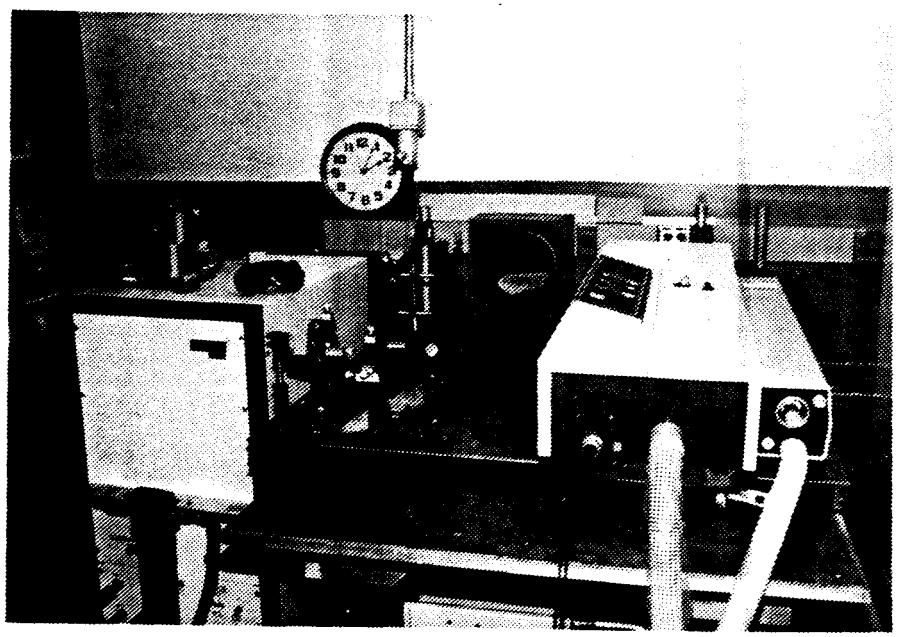

7a. Transmitter

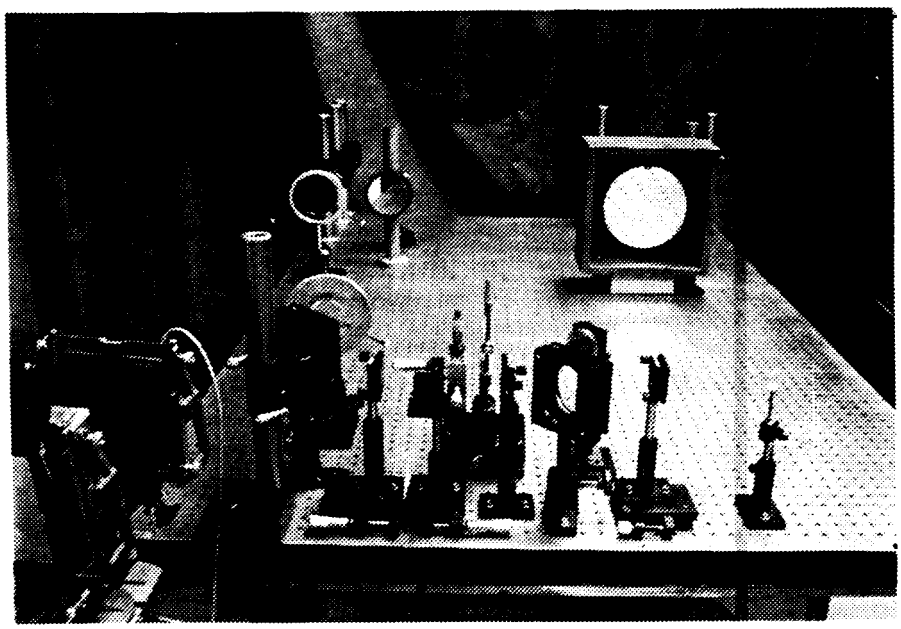

7b. Receiver

Figure 7. Photographs of the Transmitter and Receiver Optics

8a. Candle Flame

8b. Propane Torch Flame

Figure 8. Examples of Real-Time Interferograms of Simple Flow Fields

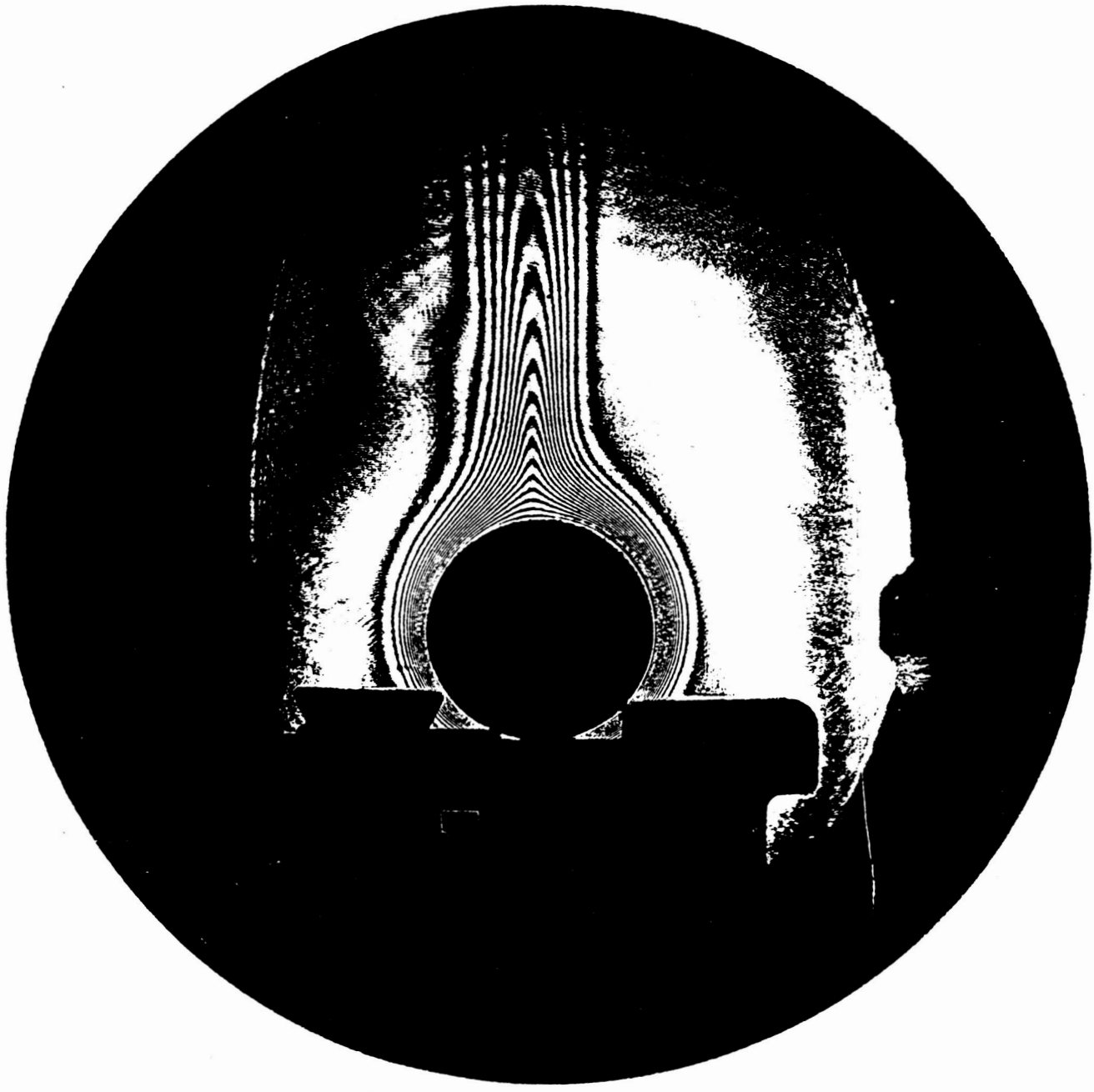

9a. Holographic Interferogram

Figure 9. Examples of Real-Time and Holographic Interferometry

9b. Point Diffraction Interferometer

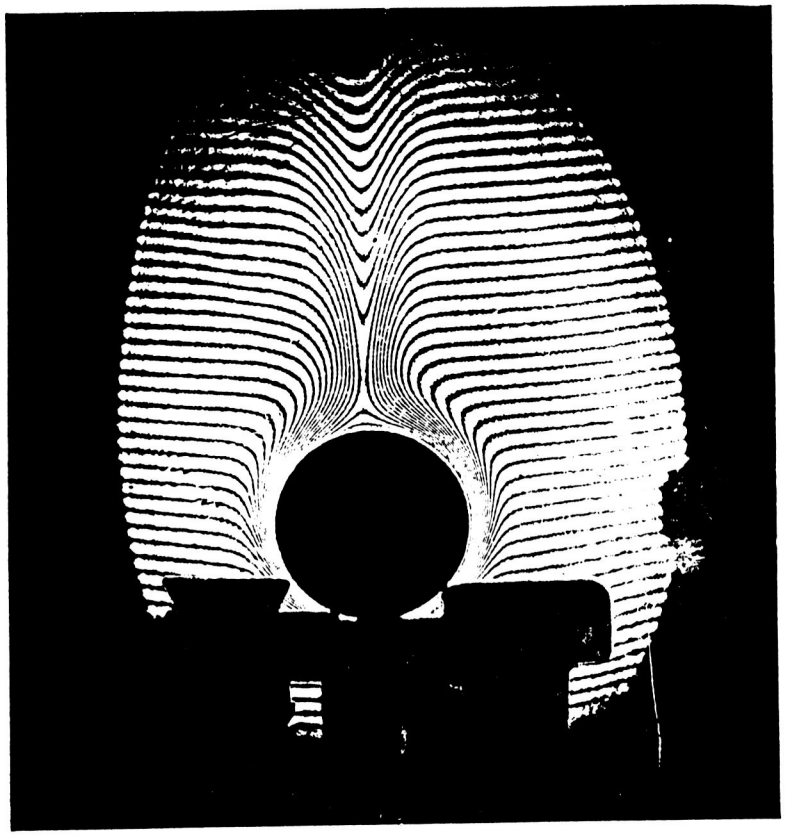

10a. Holographic

10b. Point Diffraction

Figure 10. Examples of Finite Fringe Interferograms

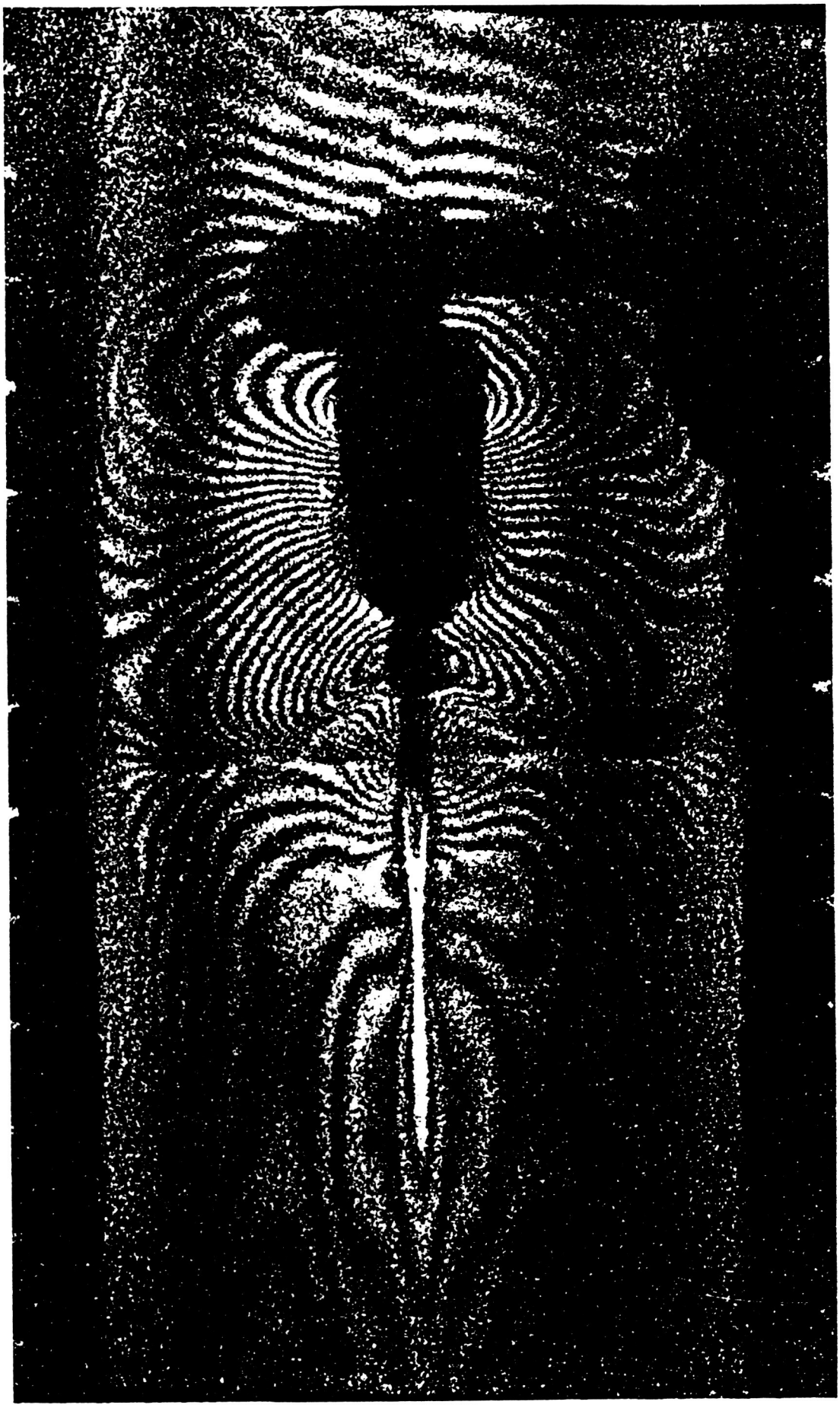

Figure 11. Interferogram of the Oscillating Airfoil

Figure 12. Interferogram of the Circulation Control Airfoil

13a. Coanda Jet Off

Figure 13. Enlargements of the Trailing Edge Flow Fields.

13b. Coanda Jet On

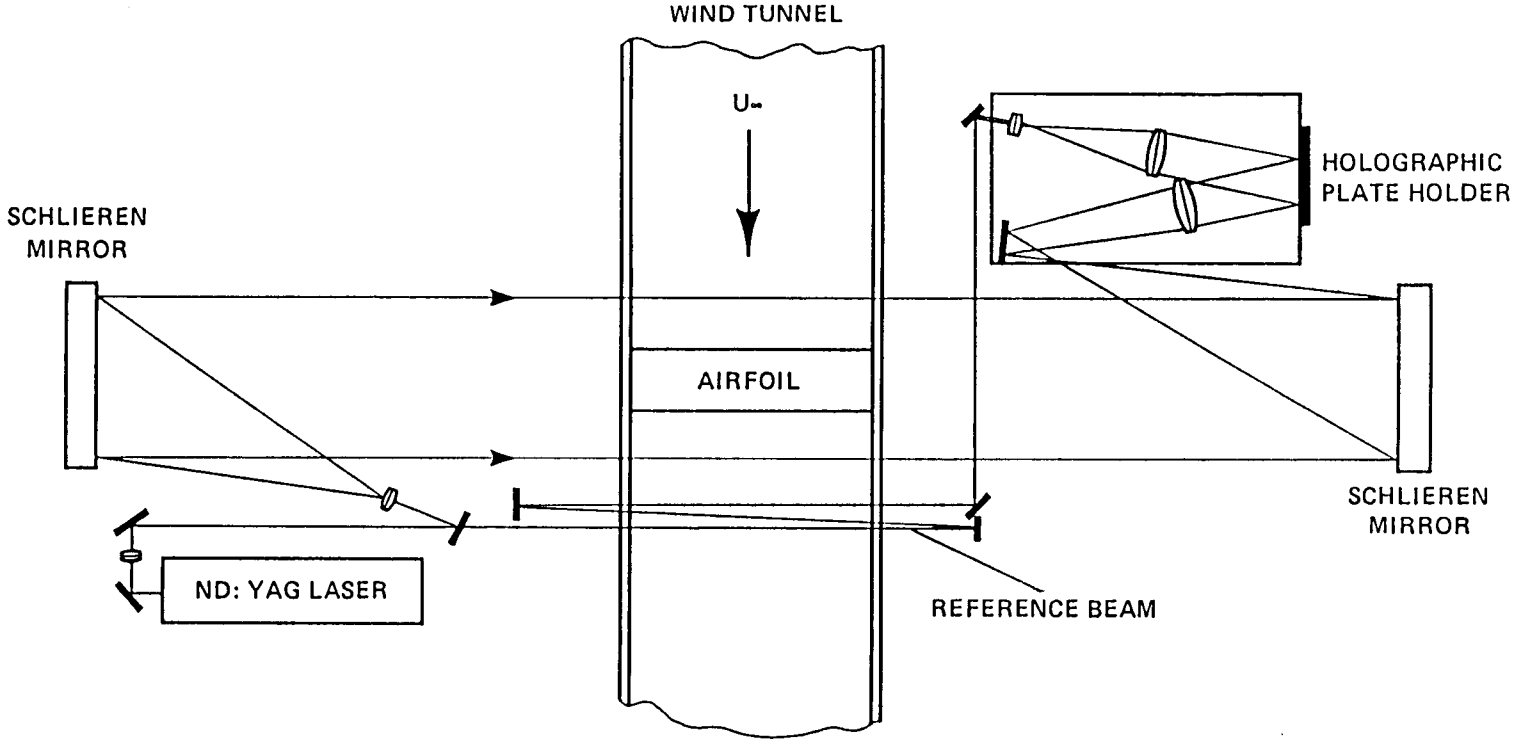

Figure 14. Holographic Interferometer Installed on the U.C. Berkeley Supersonic Wind Tunnel

Figure 15. Finite Fringe Interferogram of a Compression Corner Supersonic Flow Field

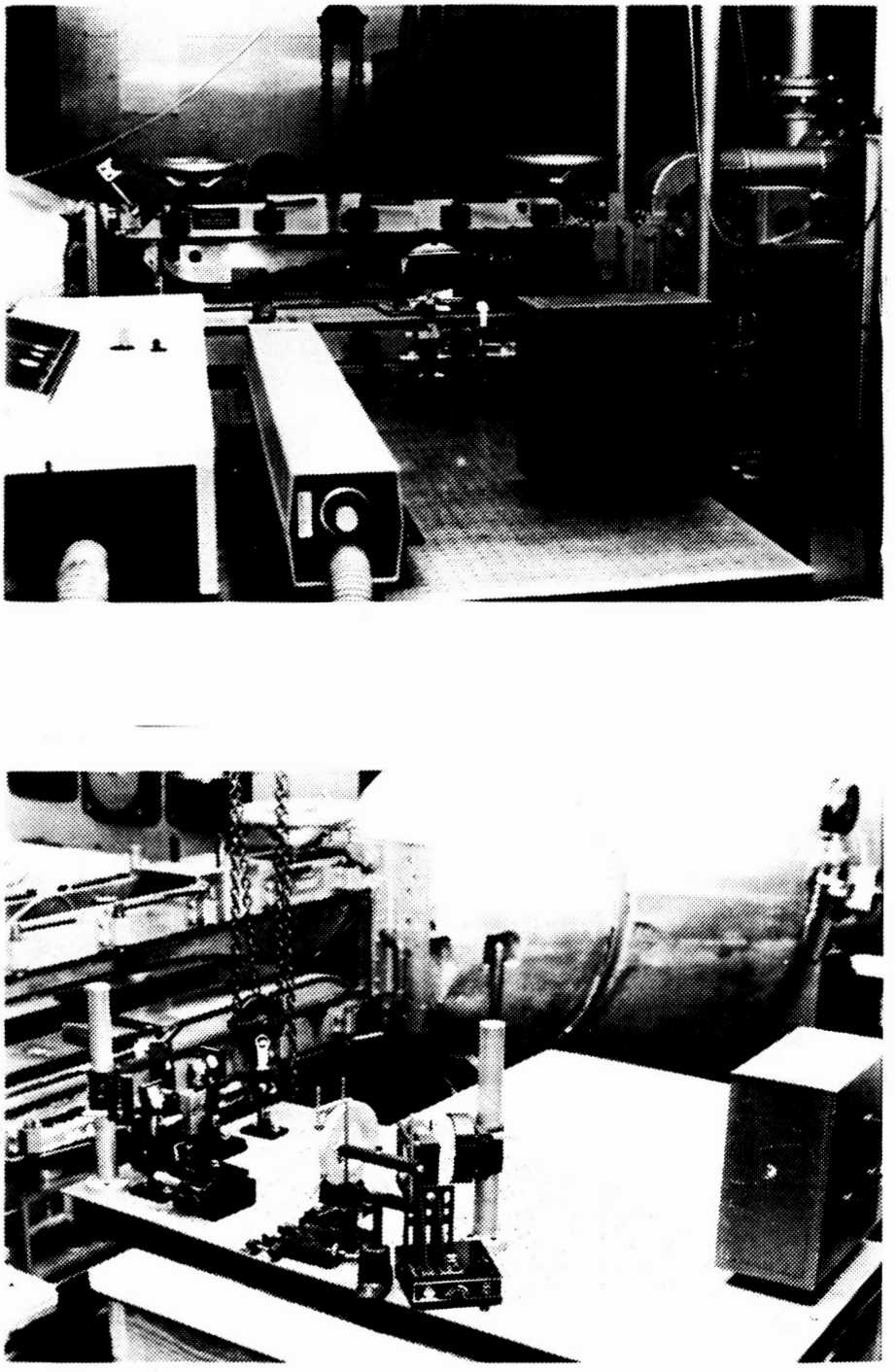

Figure 16. Point Diffraction Interferometer Installed on the U.C. Berkeley Supersonic Wind Tunnel

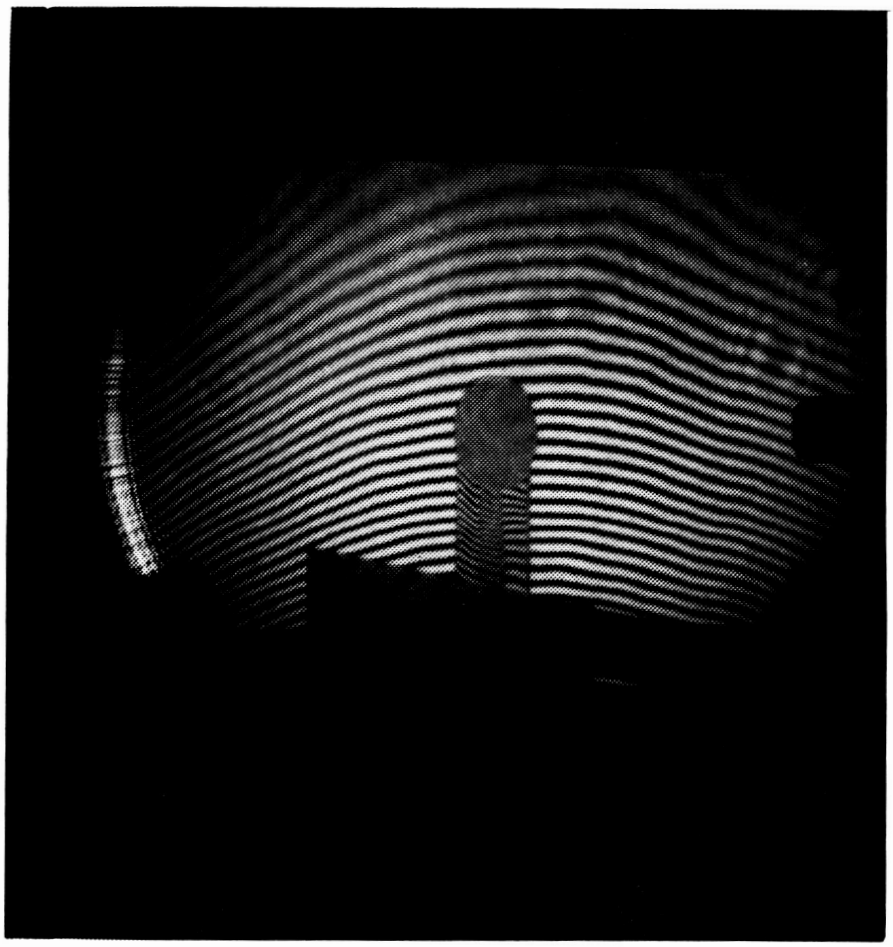

Figure 17. Example of the Fringe Patterns Produced by the Optical Imperfections in the Beam Path

NASA
National Aeronautics and Space Administration

Report Documentation Page

1. Report No.	2. Government Accession No.	3. Recipient's Catalog No.
NASA CR 177467		

4. Title and Subtitle
Evaluation and Application of a New Interferometry Technique for Compressible Flow Research

5. Report Date
October 1988

6. Performing Organization Code

7. Author(s)
William D. Bachalo
Michael C. Houser

8. Performing Organization Report No.
506-40-11

10. Work Unit No.

9. Performing Organization Name and Address
Aerometrics, Inc.
894 Ross Drive
Sunnyvale, CA 94089

11. Contract or Grant No.
NAS2-11575

13. Type of Report and Period Covered
Contractor Report

12. Sponsoring Agency Name and Address
NASA Ames Research Center
Moffett Field, CA 94035

14. Sponsoring Agency Code

15. Supplementary Notes
Point of Contact: D. A. Johnson, Ames Research Center, MS 229-1
Moffett Field, CA 94035 (415)694-5399 FTS 464-5399

16. Abstract
A new method for obtaining large scale interferograms of flow fields in real-time was investigated. The method was based upon the point diffraction interferometry technique. This method was modified to accommodate the higher laser power required in recording transonic and supersonic flow fields. Basic tests were conducted in unsteady flows and flows about circulation control airfoils at transonic speeds. It was found that vibration was not a significant factor in the application of the system. In the case of the circulation control airfoils, the real-time viewing allowed the identification of the Coanda jet interaction with the external flow and the shedding of large scale vortices. The method proved to be very sensitive to the optical quality of the wind tunnel windows. The results obtained were compared with earlier interferograms obtained using interferometry. These results were in qualitative agreemnt.

17. Key Words (Suggested by Author(s))
Interferometry
Compressible Flow
Unsteady Flow
Airfoils

18. Distribution Statement
Unlimited

Subject Category: 02

19. Security Classif. (of this report)	20. Security Classif. (of this page)	21. No. of pages	22. Price
Unclassified	Unclassified	55	A04